

Mechanical Properties of Epoxy-Based Hybrid Composites Containing Glass Beads and α,ω -Oligo(butylmethacrylate)diol

N. Schröder,^{1,*} L. Könczöl,¹ W. Döll,¹ R. Mülhaupt²

¹Fraunhofer-Institut für Werkstoffmechanik, Wöhlerstraße 11, D-79108 Freiburg, Germany

²Institut für Makromolekulare Chemie/Freiburger Materialforschungszentrum der Albert-Ludwigs-Universität, Stefan-Meier-Straße 31, D-79104 Freiburg, Germany

Received 17 January 2002; accepted 19 April 2002

ABSTRACT: A novel phase-separating liquid rubber based on oligo(alkylmethacrylate) in combination with microglass beads was used to toughen an anhydride-cured epoxy resin. The resulting hybrid composites, containing 5 or 10 wt % of oligomeric liquid rubber and between 10 and 60 wt % glass beads as well as composites containing corresponding amounts of glass beads but no liquid rubber, were characterized mechanically. The experimental data show that modification with glass beads results in increased stiffness and toughness compared to the neat resin but reduces tensile strength. Compared to the glass bead-filled compos-

ites, additional modification with methacrylic rubber leads to a further increase in toughness and also to an increase in strength but does not alter stiffness and glass-transition temperature. This synergistic behavior is explained by the fact that the rubber separates preferably on the surface of the glass bead, forming a core-shell morphology during curing. © 2003 Wiley Periodicals, Inc. *J Appl Polym Sci* 88: 1040–1048, 2003

Key words: epoxy resin; glass beads; hybrid composites; mechanical properties; toughening

INTRODUCTION

Single-phase epoxy resins exhibit high stiffness, strength, and temperature stability. Therefore these highly crosslinked materials are frequently used in many different fields of application including structural adhesives, matrix materials for fiber-reinforced composites, and encapsulation in electronic devices. Unfortunately, the high crosslink density of the network is closely associated with low crack resistance, which limits the use especially for structural applications.

Essentially, two basic concepts have been proposed to overcome the inherent brittleness of epoxy networks.¹ A well-established method to toughen epoxies is the introduction of a rubbery phase dispersed in the matrix.² This can be done either by mixing a liquid rubber with the resin/hardener system before curing, which leads to phase separation of the rubber after the gelation, or by dispersing microsized solid rubber particles in the resin.

The former method has the advantage of producing a homogeneous dispersion of rubbery particles. Although the compatibility between rubber and epoxy resin can be adjusted by applying the concept of solubility parameters, it is not easy to control the particle size. The most important liquid rubber to toughen epoxies by far is a carboxyl-terminated random copolymer of butadiene and acrylonitrile (CTBN).³ The carboxyl-end groups are able to take part in the curing reaction and consequently guarantee good adhesion between the matrix and rubber particles.

The latter method is dominated by the use of preformed core-shell particles. The particle size can be easily controlled through processing. The core thickness and polarity can be varied to adjust the compatibility with the matrix. A disadvantage of using preformed core-shell particles is the additional working step of synthesizing the particles. However, the introduction of a rubbery phase reduces stiffness and strength of the material that may affect the usability.

Another widely used method is the incorporation of inorganic fillers into the matrix.⁴ Although filling epoxies with rigid particles leads to only moderate toughness enhancement and is usually accompanied by significant strength reduction, the stiffness of the material may be strongly increased.

Although both methods have been extensively discussed in the literature, relatively few studies can be found dealing with hybrid composites modified by

*Present address: Wolff Cellulosics GmbH & Co. KG, Postfach 1662, D-29656 Walsrode, Germany.

Correspondence to: L. Könczöl (koe@iwvm.fhg.de).

Contract grant sponsor: Deutsche Forschungsgemeinschaft (DFG); contract grant number: Sonderforschungsbe- reich 428.

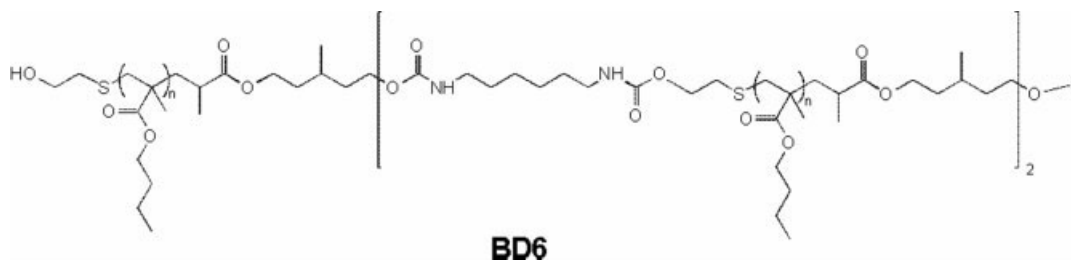


Figure 1 Chemical structure of the α,ω -oligo(*n*-butylmethacrylate)diol liquid rubber BD6.

both liquid rubber and inorganic fillers.^{5–7} The idea of combining these concepts is to link the positive effects of each single concept such as enhancement of both toughness and stiffness and to minimize negative effects such as reductions in strength and temperature behavior.

Based on a previous study⁸ characterizing the mechanical properties of an epoxy resin toughened with α,ω -oligo(*n*-butylmethacrylate)diol (BD), which was recently developed by Fock et al.,⁹ the present work examines the properties of an epoxy resin filled with various amounts of microglass beads and additionally modified with BD. Although the glass-transition temperatures of methacrylic oligomers are not as low as that of CTBN, the temperature stability of methacrylics is considered to be better than that of oligomers containing unsaturated bonds in the oligomer backbone.

EXPERIMENTAL

Materials

The base resin Araldite GY 250 used in this investigation is a low-molecular-weight viscous diglycidylether of bisphenol-A (DGEBA), supplied from Ciba Geigy AG (Basel, Switzerland). Its functionality is 5.3 mmol epoxide per g, as determined by titration according to standard DIN 16945. Hexahydrophthalic acidanhydride (HHPA) HT 907 (Ciba-Geigy) was used as a curing agent in combination with *N,N*-dimethylbenzylamine (DBA) DY 062 (Ciba-Geigy) as an accelerator. All components were used as received.

The elastomeric modifier used in this study was synthesized by chain extension of BD, characterized by a molar mass of 2000 g/mol (BD2). BD2 was supplied from Th. Goldschmidt AG (Essen, Germany) as a technical product solved in acetone. The chain extension was performed by hexamethylenediisocyanate-mediated urethane coupling. Details of this reaction and the spectroscopic characterization of the coupling products are described elsewhere.⁸ The material used in this investigation, denoted as BD6 (Fig. 1), is a telechelic BD2-coupling product characterized by a molar mass of 5100 g/mol (measured by vapor pressure osmosis). DSC measurements on BD6, applying a

heating rate of 20 K/min, reveal a glass-transition temperature of -1°C . To facilitate handling by lowering viscosity, BD6 was solved in a defined amount of acetone.

Solid microglass beads (GP) without any surface treatment (Potters Ballotini, Kirchheimbolanden, Germany) were used as an inorganic filler. The glass is a borosilicate glass consisting of SiO_2 , B_2O_3 , Al_2O_3 , and other alkali and chalcogen oxides. The glass microspheres, having an average diameter of $6.5\ \mu\text{m}$, were washed with ethanol and vacuum-dried at 80°C for 24 h before use.

To prepare the hybrid composite material, DGEBA was mixed with BD6 solution to produce the desired rubber concentrations. After completely removing the acetone, 0.92 mol HHPA per mol epoxide was added. A homogeneous mixture was obtained that was degassed in vacuum at 80°C until all air bubbles had disappeared. The mixture was poured into a standardized tin and an appropriate amount of glass beads was added to produce the desired composition. The mixture was manually stirred for 1 min and then placed into a special high speed vacuum mixer. Mixing was performed in vacuum at 90°C until a homogenous dispersion was obtained. Before pouring the mixture into a release agent-treated steel mold sheet preheated to 90°C , 0.018 mol DBA per mol epoxide was added and solved by gentle stirring for another 3 min.

Curing was performed in an air-circulating oven for 3 h at 150°C followed by 1 h at 180°C . Before removing the mold sheet from the oven it was allowed to cool to room temperature.

As reference systems glass bead-filled epoxies without addition of BD6 were prepared in an analogous way as described above. Denotation and modifier content of all materials used in this study are given in Table I.

Testing methods

The cured materials were examined by a variety of different techniques. Short-term tensile properties such as tensile strength and Young's modulus were measured according to standard DIN 53455 in an Instron 4204 servohydraulic testing machine using dog-

TABLE I
Materials Synthesized and Characterized in This Study

Denotation	Content of liquid rubber (BD6) (wt %)	Content of glass beads (GP) (wt %)
Neat resin	0	0
5BD6	5	0
10BD6	10	0
15BD6	15	0
10GP	0	10
20GP	0	20
40GP	0	40
60GP	0	60
5BD610GP	5	10
5BD620GP	5	20
5BD630GP	5	30
5BD640GP	5	40
5BD660GP	5	60
10BD620GP	10	20

bone-shaped tensile bars (4 mm thickness, 10 mm width, and 60 mm gauge length), which were cut out of the composite sheets. The tensile experiments were performed at a crosshead speed of 5 mm/min. A strain gauge extensometer was applied for strain measurement. Young's modulus E was taken from the slope of the initial linear region of the measured stress–strain curve at 0.1% strain.

Creep tests were performed in a Frank creep testing system in which up to 15 tensile specimens can be loaded individually at constant loads. The loading device of each specimen is equipped with digital clocks, which indicate the loading time to an accuracy of 1/100 of an hour and have a circuit breaker to stop the clocks upon specimen failure. The specimens used were similar to those used in short-term tensile experiments. The lifetimes of the specimens were plotted versus the individual stress applied on a double-logarithmic scale.

Fracture toughness K_{Ic} was determined by tensile experiments on saw-notched compact-tension (CT) specimens in a Zwick tensile testing machine (Zwick, Germany) at a crosshead speed of 1.8 mm/min. The dimensions of the CT specimens were thickness $B = 4$ mm, height $2H = 8$ mm, and effective width $W = 8$ mm. Before testing, the precrack was sharpened by pushing a razor blade into the saw notch. The effective crack length a was measured after testing using a traveling microscope. The maximum load P_c measured in the experiment was taken to calculate K_{Ic} according to eq. (1):

$$K_{Ic} = \frac{P_c(2W + a)}{[B(W - a)]^{3/2}} Y\left(\frac{a}{W}, \frac{H}{W}\right) \quad (1)$$

The geometric factor $Y[(a/W), (H/W)]$, valid for CT specimens, was calculated according to Srawley and Gross.¹⁰

Dynamic mechanical analysis (DMA) was performed using a Rheometrics RSA II Solids Analyzer (Rheometrics, Poole, UK) equipped with a dual-cantilever specimen mounting tool. A frequency of 1 Hz and a strain level of 0.1% were applied to record the storage modulus E' as well as the loss factor $\tan \delta$, scanning a temperature range from -120 to 160°C at a heating rate of 3 K/min. The dimensions of the specimens were $50 \times 4 \times 3 \text{ mm}^3$. The maximum energy loss (i.e., the α -peak maximum of the $\tan \delta$ versus T graph was taken as an approximation of the glass-transition temperature T_g of the tested materials).

Some fracture surfaces of the tensile test specimens were examined by scanning electron microscopy (SEM) using a CamScan electron microscope (Cambridge Instruments, Cambridge, UK) operating at an accelerating voltage of 25 kV. To prevent charging of the samples and to protect the surface structures, the surfaces were coated with copper metal using a low energy sputtering process.¹¹

RESULTS AND DISCUSSION

Modulus and strength are key properties that basically decide the suitability of a material for usage in structural applications. Figure 2 shows the tensile modulus as a function of both liquid rubber content and microsphere content for epoxy resins modified with different amounts of glass beads and of BD6. Starting from 2.9 GPa for the neat resin, the modulus progressively increases with microsphere content whereas it decreases with increasing rubber content. Comparing the moduli of filled resins with and without additional modification with liquid rubber (5% BD6) up to 40 wt % microsphere content, as shown in Figure 3, the values of corresponding resins in both series differ only marginally, which shows that the additional content of the low modulus rubber BD6

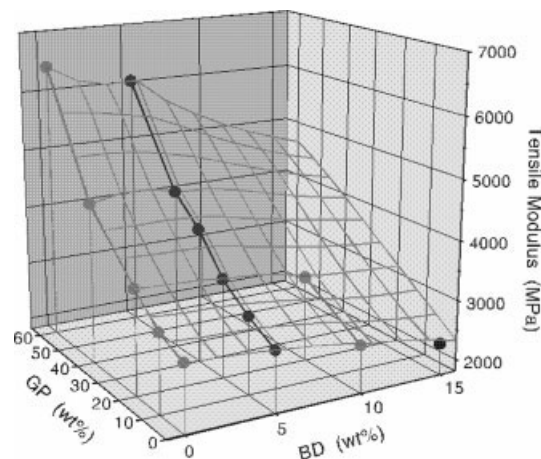


Figure 2 Tensile modulus E of differently modified epoxy composites as a function of rubber (BD) and glass bead (GP) contents: measured data (●) with graphic extrapolation.

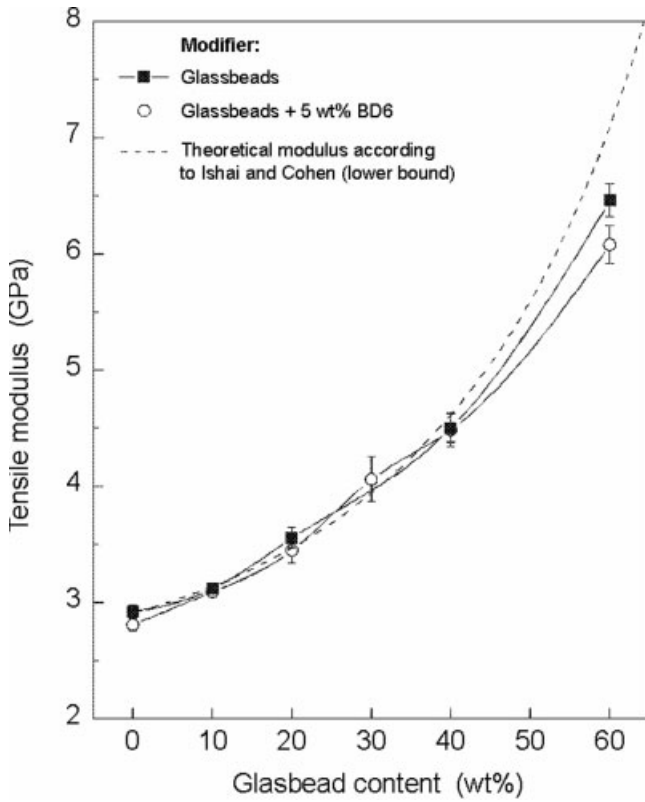


Figure 3 Tensile modulus E of glass bead-filled epoxy composites with and without additional rubber modification (5 wt % BD6) versus glass bead contents.

does not significantly influence the composite stiffness. Only at a microsphere content as high as 60 wt % does the additional BD6 content lower the tensile modulus about 0.4 GPa compared to that of the corresponding GP-series composite.

Various theories have been developed to explain dependency of the modulus on the filler particle content of composites. One approach is the lower-bound model of Ishai and Cohen,¹² which assumes cubic particles surrounded by a matrix shell and a uniform displacement applied to the boundary of the particles and leads to eq. (2), where V_p is the volume fraction of particles, E_c is the composite modulus, E_0 is the matrix modulus, and E_p is the particle modulus.

$$E_c = E_0 \left[1 + V_p \left(\left(\frac{E_p/E_0}{(E_p/E_0)^{-1}} \right) - V_p^{1/3} \right)^{-1} \right] \quad (2)$$

Fitting the model by taking the neat resin's experimentally determined modulus of 2920 MPa as E_0 and the glass bead's modulus of 75 GPa (as given by the manufacturer) as E_p , and using the microsphere content V_p as converted from wt %, the broken curve shown in Figure 3 results. There is a good agreement between the model and the experimental data up to glass bead contents of 40 wt %, as was also observed by other investigators.^{7,13,14}

The increase in modulus attributed to the addition of glass beads can also be seen in Figure 4, which shows storage modulus E' and $\tan \delta$ of neat and modified epoxy resins (modified with 5 wt % of BD6 and 40 wt % of GP) as functions of temperature. Below as well as above the glass-transition temperature T_g , the storage modulus of the modified resin is significantly higher than that of the neat resin. As also found by Ebdon et al.,¹⁵ the T_g is scarcely affected by the addition of glass beads (Table II). Although modifying with 5 wt % lowers the T_g by approximately 3 K compared to that of the neat resin, even slightly increasing the glass bead content increases T_g with respect to the BDGP-series resins. As can be seen in Table II, modifying with 5 wt % BD6 and 40 wt % glass beads leads to a 5 K increase of T_g compared to that of a resin modified with 5 wt % BD6. This effect was also observed in other filled epoxy systems in which the filler was well bonded to the matrix^{7,16} but is usually not found in filled composites without strong filler-matrix interactions. According to Landel¹⁷ the adhesion effect between the filler surface and the surrounding matrix results in an immobilization of the latter, which should be promoted by increasing the filler-matrix adhesion. Lowering the matrix flexibility directly increases the glass-transition temperature. Comparing the T_g values of the GP-series resins and the

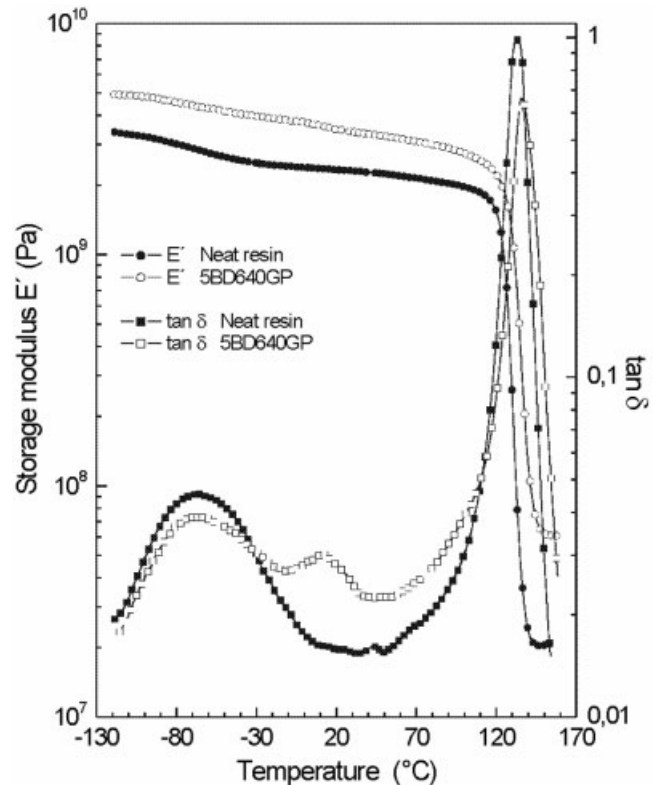


Figure 4 Storage modulus E' and loss factor $\tan \delta$ of the neat epoxy resin and of a hybrid composite with 5% rubber and 40% glass bead contents.

TABLE II
Glass-Transition Temperature of GP-Series Resins
and BDGP-Series Resins

Material	T_g (°C)
Neat resin	133
5BD6	130
10BD6	128
15BD6	126
10GP	133
20GP	134
40GP	134
60GP	135
5BD610GP	132
5BD620GP	133
5BD630GP	134
5BD640GP	135
5BD660GP	135
10BD620GP	130

BDGP-series resins suggests that the glass bead–matrix adhesion in the hybrid composites is increased compared to that of the glass bead composites. This result points to the possibility that the additional BD6 content promotes adhesion between the glass bead surface and the matrix.

The short-term tensile strength σ_B of the differently modified resins is shown in Figure 5 as a function of microsphere and rubber content. For better understanding, it is represented in two different perspectives, the same as in Figure 2 [Fig. 5(a)] and turned by 180° [Fig. 5(b)]. Although the neat resin exhibits a tensile strength of 87.6 MPa, the addition of only 10 wt % glass beads decreases σ_B by 22% compared to that of the neat resin. At a glass bead content of 60 wt % the composite exhibits a tensile strength of 41.1 MPa, which is only 47% of the neat resin's strength. Additional modification with BD6 significantly moderates this strength decrease. A hybrid composite containing 60 wt % glass beads and 5 wt % BD6 shows a tensile strength of 53.0 MPa, which is about 29% more than the strength of the corresponding glass bead composite. Regarding these results from another point of view, it can be stated that modification of a glass bead composite with 5 wt % BD6 results in a strength *increase* of 12 to 30% compared to that of the glass bead composite, although modification of the resin with BD6 only results in a *decrease* in strength; for example, at a rubber content of 5% the strength decreased by about 7% compared to that of the neat resin.

This surprising result can be explained by comparing the fracture surfaces of a glass bead composite and the corresponding hybrid composite. Micrographs of the fracture surface of a glass bead–modified composite containing 20 wt % glass beads are shown in Figure 6(a), (b). It can be seen clearly that the glass beads are isolated from the matrix. A strong surface energy mismatch of glass beads and matrix in combination with

the absence of reactive chemical groups on the glass bead surfaces leads to interface incompatibility and thus to poor adhesion between the glass bead surfaces and the surrounding matrix. Upon loading, the glass beads are completely debonded from the matrix, the bead surfaces show only very few traces of epoxy resin, and gaps up to 500 nm are formed between the matrix and the particle surfaces. Micrographs taken from the fracture surface of the corresponding hybrid composite containing 20 wt % microspheres and 5 wt % BD6 [Fig. 7(a), (b)] give a completely different picture. The glass beads are well bonded to the matrix, and the surfaces of the glass beads are not visible because of complete coverage with matrix and separated rubber. Gaps between the matrix and microspheres are absent. The rubbery modifier BD6 has precipitated from the resin upon curing and is distributed in the matrix as small particles with diameters of about 600 nm. Moreover, Figure 7(a) indicates that the

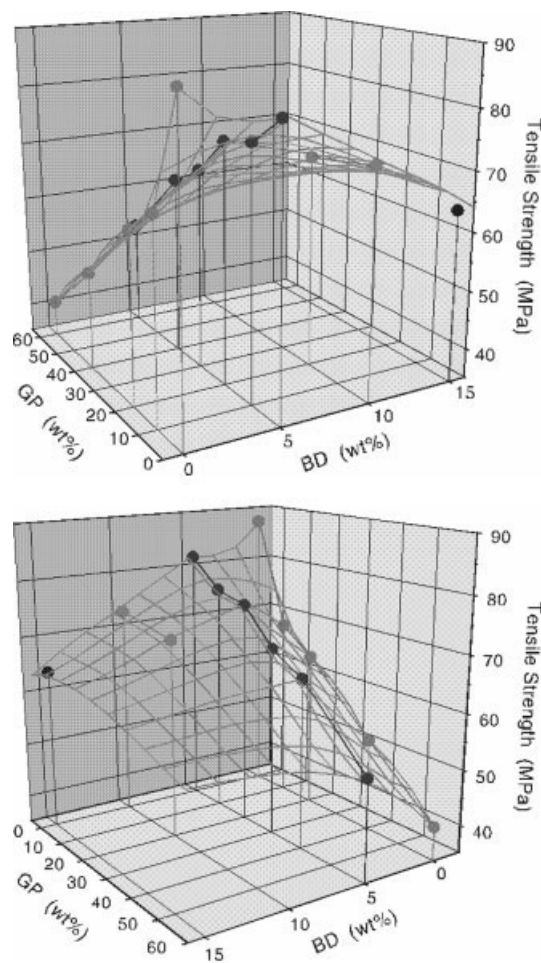
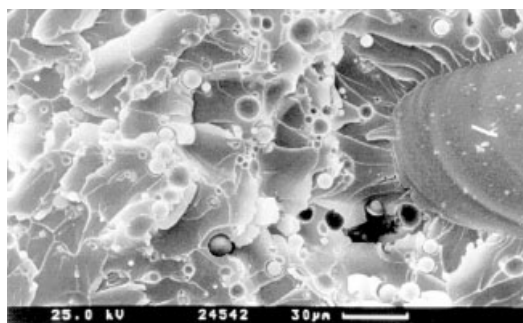


Figure 5 Tensile strength σ_B of differently modified epoxy composites as a function of rubber (BD) and glass bead (GP) contents [measured data (●) with graphic extrapolation]: (a) with GP content as x -axis and BD content as y -axis (as in Fig. 2); (b) with BD content as x -axis and GP content as y -axis [(a) turned by 180°].



(a)



(b)

Figure 6 SEM micrographs of (a) fracture surface in glass bead-filled epoxy resin (20 wt % GP) with glass beads separated from the epoxy matrix; (b) detail of (a) at a higher magnification.

area density of these rubbery particles located on the glass bead surface is significantly higher than that in the matrix. Furthermore, the BD6 particles sticking to the glass bead surface are about twice as large as the particles distributed in the matrix.

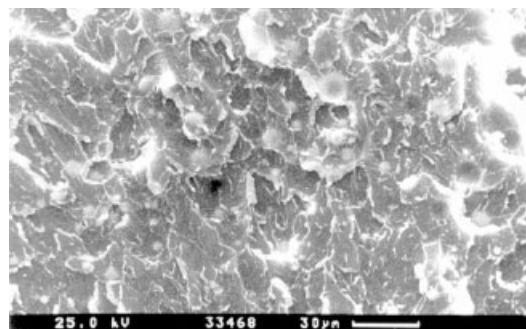
Regarding the chemical structure of BD6 (Fig. 1), it is proposed that the polarity of this molecule is quite high because of the large number of ester groups attached to the oligomer backbone. Assuming strong interactions between these ester groups and the polar glass bead surfaces, an accumulation of BD6 on the glass bead surfaces in the very early stage of curing is quite reasonable, resulting in the morphology shown in Figure 7(a). X-ray emission spectroscopy can be used to prove the nature of the particles sticking on the glass beads (Fig. 8). The solid curve shown in Figure 8 results from scanning the neat glass bead surface in Figure 6(b). The spectrum shows three peaks related to the elements Si, Cl, and Ca, which are typical components of glass. The broken curve, on the other hand, shows the spectrum resulting from scanning the covered glass bead shown in Figure 5(b). In addition to the elements Si, Cl, and Ca, a fourth peak corresponding to the element S appears. This peak directly proves that the material sticking to the glass bead is mostly BD6 because BD6 is the only resin system component containing sulfur (Fig. 1). It can

thus be concluded that BD6 works as an *in situ* compatibilizer that improves adhesion between matrix and glass beads, also resulting in the improved fracture strength of hybrid composites compared to that of glass bead composites. With regard to glass bead composites, this result indicates that the additional treatment of glass beads with a silane coupling agent to improve adhesion might be obsolete in combination with the given liquid rubber because this effect can be generated as well simply by the addition of small amounts of BD6.

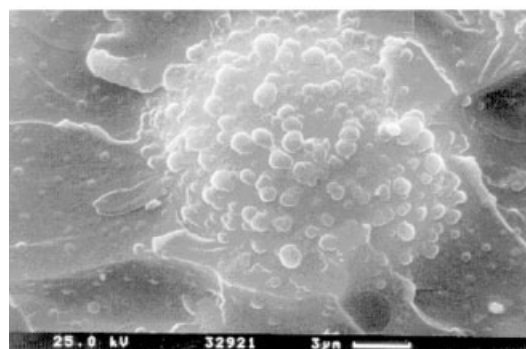
Fracture strength improvement of glass bead composites by additional modification with BD6 can also be revealed in long-term tensile experiments. In Figure 9 the tensile stress applied to specimens of different materials is plotted as a function of the time to fracture t_f (i.e., the lifetime) on a double-logarithmic scale, where each data point corresponds to the mean value of two individual measurements. Fitting the data according to eq. (3) results in a straight line with intersection A and slope s for each material. The parameters A and s are listed in Table III.

$$\log \sigma = \log A + s \log t_f \quad (3)$$

The parameters A and s can be derived from short-term properties to characterize the long-term strength



(a)



(b)

Figure 7 SEM micrographs of (a) fracture surface in a hybrid composite (with 5% BD and 20 wt % GP) with glass beads covered with a layer of liquid rubber; (b) detail of (a) at a higher magnification.

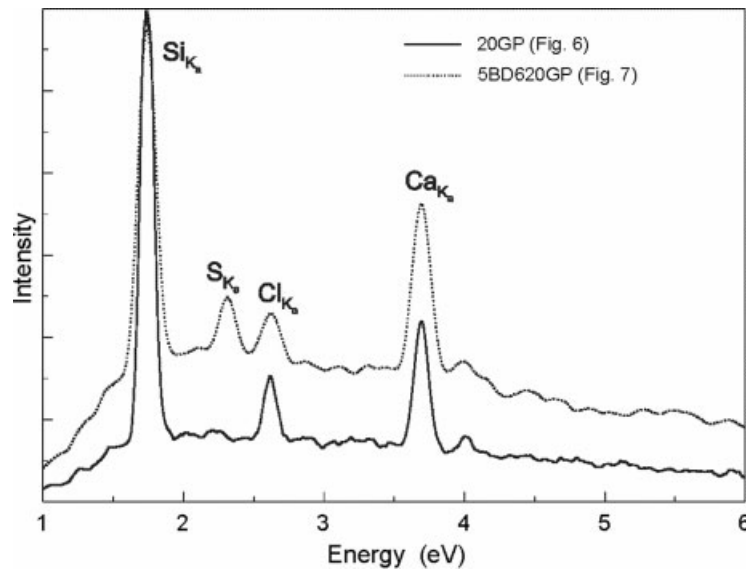


Figure 8 X-ray emission spectra (EDX) of glass beads in the modified epoxies in Figures 6 and 7.

properties of a material enabling lifetime predictions of brittle polymers.^{18,19} The slope s indicates the stress sensitivity of the material, whereas A represents the short-term strength and should be equal to σ_B . This holds for all materials of Table III within a deviation of 8%.

As can be seen from Figure 9 and Table III the slope of the lifetime functions of the composites containing glass beads is slightly steeper than of the neat resin. The short-term strength of the glass bead-filled composites is much lower than that of the unfilled resins. However, it is remarkable that the strength of the composites without additional rubber content is significantly lower than the corresponding values of the hybrid composites that also result in substantial dif-

ferences in long-term strength. Applying a load of 60% of A the resin filled with 20% of GP will break after approximately 5 to 6 days, whereas the resin modified additionally with 5% of BD6 will last more than 7 times as long.

In Figure 10 the fracture toughness K_{Ic} is shown as a function of both microsphere and rubber contents for the differently modified resins. The addition of 10 wt % GP as well as modifying with 5 wt % BD6 approximately doubles K_{Ic} from 0.56 MPa $\cdot\sqrt{m}$ for the neat resin to 1.09 MPa $\cdot\sqrt{m}$. A further increase of glass bead content results in increasing K_{Ic} values in both series, although the curve that results from fitting the hybrid composite data is located well above the corresponding curve for the filled resins without rubber

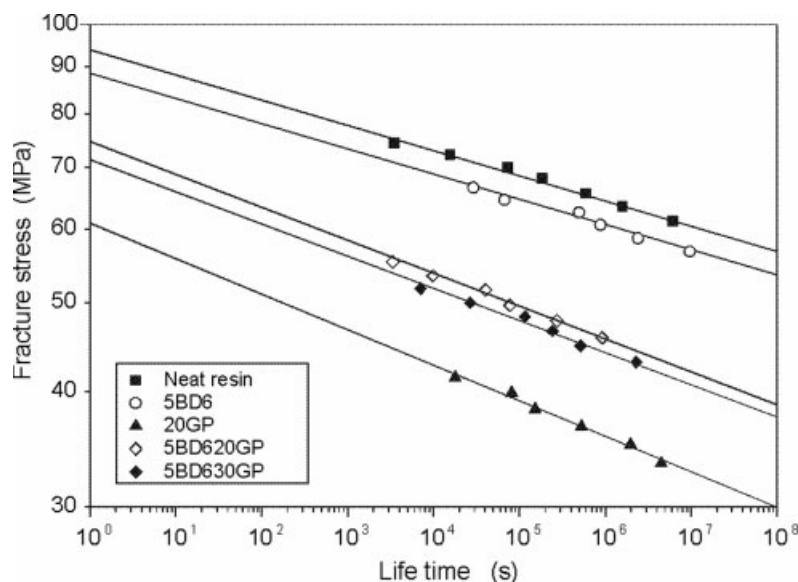


Figure 9 Fracture stress σ_B versus time to fracture (lifetime t_L) of differently modified epoxy resins.

TABLE III
Short-Term Fracture Strength σ_B and Long-Term
Experiment Parameters A and s of Eq. 3, Calculated
from Fitting the Data of Figure 8

Material	σ_B (MPa)	A (MPa)	s
Neat resin	87.6	93.5	-0.027
5BD6	81.9	88.0	-0.027
20GP	63.8	61.0	-0.039
5BD620GP	75.4	73.3	-0.034
5BD630GP	69.0	69.7	-0.033

content. Whereas the slope of the curve for the hybrid resins slightly decreases with increasing glass bead content, the slope of the GP-series curve strongly decreases with increasing glass bead content. Therefore the toughness difference between the two series of filled resins increases with increasing glass bead contents.

The approximately additive partial toughness contributions of the individual types of modifier used to toughen the hybrid resins can be explained by considering the fact that glass beads and microsized rubber particles dispersed in a brittle matrix induce different energy dissipation mechanisms that affect crack loading and crack propagation, respectively. The toughening mechanism effective in glass bead-filled resins and other particle-filled polymers is crack pinning, originally proposed by Lange²⁰ and now generally accepted in the literature.^{21,22} The crack front is pinned to the particles in front of the propagating crack and is thus bowed between adjacent particles, resulting in an enlargement of the fracture surface and subsequently also to an increased energy dissipation. In most cases this process is accompanied by the formation of steps on the fracture surface behind the particles, leveling upon reunification of the crack front. On micrographs these steps can be identified as lancets that start at the

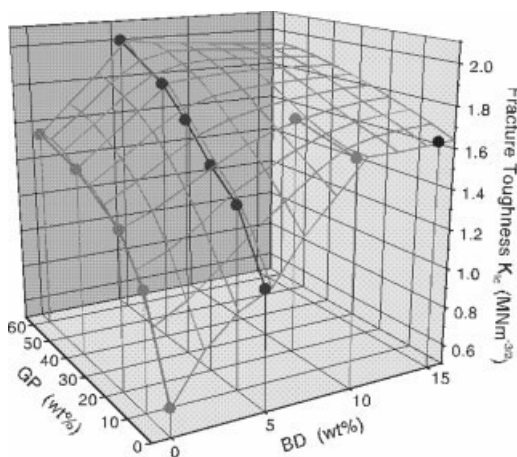


Figure 10 Fracture toughness K_{Ic} of differently modified epoxy composites as a function of rubber (BD) and glass bead (GP) contents: measured data (●) with graphic extrapolation.

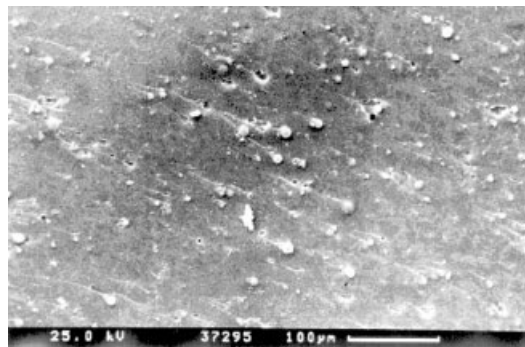


Figure 11 SEM micrograph of a fracture surface in a hybrid epoxy composite (with 5% BD6 and 10 wt % GP) exhibiting lancets starting from glass beads.

particle and point in the direction of the propagating crack. This is demonstrated in Figure 11, which shows a micrograph of a fracture surface of a hybrid composite modified with 5 wt % BD6 and 10 wt % glass beads. Rubber particles, on the other hand, are subjected to cavitation in the process zone in front of the crack tip, which promotes localized shear yielding of the surrounding matrix. The fracture surface of a resin modified with 5 wt % BD6 (Fig. 12) shows that cavitation processes are possible, although the glass temperature of BD6 is only 20 to 25°C lower than room temperature. Both mechanisms, crack pinning and cavitation combined with matrix shear yielding, can operate independently without significant interference. This enables further improvement in toughness of glass bead composites by additional modification with relatively small amounts of BD6.

Another parameter that characterizes the material's toughness is the critical energy release rate G_{Ic} . Assuming plain strain conditions, G_{Ic} can be calculated from tensile modulus E , critical stress intensity factor K_{Ic} , and Poisson ratio ν in the following equation:

$$G_{Ic} = \frac{K_{Ic}^2}{E} (1 - \nu^2) \quad (4)$$

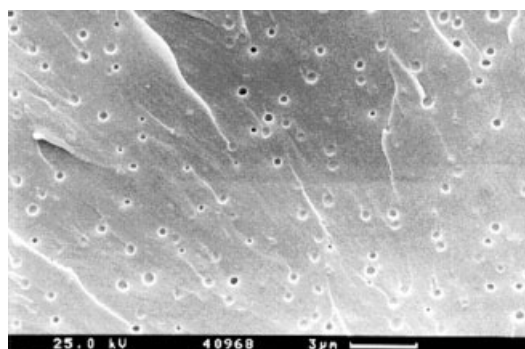


Figure 12 SEM micrograph of a fracture surface in a rubber-toughened epoxy (with 5% BD6) exhibiting cavitation of the rubber particles.

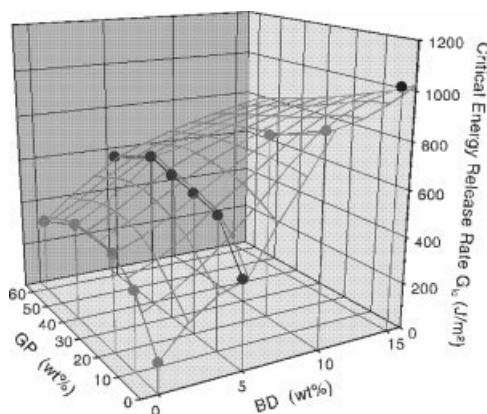


Figure 13 Critical energy release rate G_{Ic} of differently modified epoxy composites as a function of rubber (BD) and glass bead (GP) contents: measured data (●) with graphic extrapolation.

Figure 13 shows G_{Ic} as function of glass bead content for the glass bead-filled resins and the hybrid resins, assuming $\nu = 0.35$. For the resins of both series G_{Ic} exhibits a maximum located at approximately 30 wt % of glass beads for the GP series and at approximately 40 wt % for the hybrid resins. This type of function is frequently found in glass bead-filled epoxy resins and is attributed to the fact that the increase of K_{Ic} with increasing glass bead content is degressive, whereas the increase of E is progressive with increasing glass bead contents. A resin modified with 40 wt % glass beads exhibits a G_{Ic} value of 420 kJ/m², which is an increase of 230% compared to the neat resin with $G_{Ic} = 125$ kJ/m². Modification with 40 wt % glass beads and 5 wt % BD6 leads to a G_{Ic} value of as much as 670 kJ/m², which represents an increase of 60% compared to that of the resin filled with 40% GP and 430% compared to that of the neat resin.

CONCLUSIONS

Improved toughness of polymers is usually connected with deterioration of other material properties such as strength and stiffness. This also holds for epoxy resins modified with α,ω -oligo(*n*-butylmethacrylate)diol. On the other hand, polymers filled with inorganic fillers such as glass beads combine toughness and stiffness improvements but exhibit even lower strength, as was also shown in this study.

However, the toughness of hybrid composites containing both α,ω -oligo(*n*-butylmethacrylate)diol as a liquid rubber and glass beads as filler is higher than the toughness of both glass bead-filled epoxies and rubber-toughened epoxies. The toughness gain compared to that of neat resin is almost as high as the sum

of the individual toughness improvements. The stiffness of hybrid composites is similar to the stiffness of glass bead-filled epoxies. There is a negligible stiffness reduction attributed to liquid rubber. The strength of the hybrid composites is improved significantly compared to the strength of glass bead-filled epoxies.

The significant toughness improvement is attributed to the combination of the toughening mechanisms resulting from both rigid particles and phase-separated rubber particles in the epoxy matrix. The mechanism leading to the synergistic behavior has been found to be the formation of a surface layer of α,ω -oligo(*n*-butylmethacrylate)diol on the glass beads during curing, which creates a core-shell morphology.

The authors thank the Deutsche Forschungsgemeinschaft (DFG) for support of the investigations described in this report through Sonderforschungsbereich 428.

References

- Mülhaupt, R. In *Toughened Thermoplastics and Thermosets*; Brostow, W., Ed.; Performance of Plastics; Hanser: Munich, 2000; Chapter 20, pp 487–518.
- Bucknall, C. B. *Toughened Plastics*; Applied Science Publishers: London, 1977.
- Bandyopadhyay, S. *Toughened Plastics, I*; ACS Symposium Series 233; American Chemical Society: Washington, DC, 1993; p 221.
- Johnston, N. J., Ed. *Toughened Composite*, ASTM STP 937; Philadelphia, 1987.
- Moloney, A. C.; Kausch, H. H.; Kaiser, T.; Beer, H. R. *J Mater Sci* 1987, 22, 381.
- Young, R. J.; Maxwell, D. L.; Kinloch, A. J. *J Mater Sci* 1986, 21, 380.
- Maazouz, A.; Sautereau, H.; Gerard, J. F. *J Appl Polym Sci* 1993, 50, 615.
- Schröder, N.; Könczöl, L.; Döll, W.; Mülhaupt, R. *J Appl Polym Sci* 1998, 70, 785.
- Esselborn, E.; Fock, J.; Knebelkamp, A. *Macromol Symp* 1996, 102, 91.
- Srawley, J. E.; Gross, B. *Eng Fract Mech* 1972, 4, 587.
- Schinker, M. G.; Könczöl, L.; Döll, W. *J Mater Sci Lett* 1982, 1, 475.
- Ishai, O.; Cohen, L. J. *Int J Mech Sci* 1967, 9, 539.
- Xu, A.-R.; Nishino, T.; Nakamae, K. *Polymer* 1992, 33, 5167.
- Amdouni, N.; Sautereau, H.; Gerard, J. F. *J Appl Polym Sci* 1992, 46, 1723.
- Ebdon, M. P.; Delatycki, O.; Williams, J. G. *J Polym Sci Part B: Polym Phys* 1974, 12, 1555.
- Manson, J. A.; Chiu, E. H. *J Polym Sci* 1973, 41, 95.
- Landel, R. F. *Trans Soc Rheol* 1958, 2, 53.
- Döll, W.; Könczöl, L. *Kunststoffe* 1980, 70, 563.
- Beer, H. R.; Kaiser, T.; Moloney, A. C.; Kausch, H. H. *J Mater Sci* 1986, 21, 3661.
- Lange, F. F. *Philos Mag* 1970, 22, 983.
- Moloney, A. C.; Kausch, H. H.; Stieger, H. R. *J Mater Sci* 1983, 18, 208.
- Moloney, A. C.; Kausch, H. H.; Stieger, H. R. *J Mater Sci* 1984, 19, 1125.